Resonant Nernst Effect in the Metallic and Field-Induced Spin Density Wave States of $(TMTSF)_2ClO_4$

E. S. Choi,[1] J. S. Brooks,[1] H. Kang,[2] Y. J. Jo,[2] and W. Kang[2]
[1]*NHMFL/Physics, Florida State University, Tallahassee, Florida 32310, USA*
[2]*Department of Physics, Ewha Womans University, Seoul 120-750, Korea*
(Received 26 January 2005; published 25 October 2005)

We examine an unusual phenomenon where, in tilted magnetic fields near magic angles parallel to crystallographic planes, a ''giant'' resonant Nernst signal has been observed by Wu *et al.* [Phys. Rev. Lett. **91**, 056601 (2003)] in the metallic state of an organic conducting Bechgaard salt. We show that this effect appears to be a general feature of these materials and is also present in the field-induced spin density wave phase with even larger amplitude. Our results place conditions on any model that treats the metallic state as a state with finite Cooper pairing.

DOI: 10.1103/PhysRevLett.95.187001 PACS numbers: 74.70.Kn, 72.15.Gd, 72.15.Jf, 75.30.Fv

The Bechgaard salts, $(TMTSF)_2X$ ($X = PF_6$, ClO_4, AsF_6, ReO_4, etc.), continue to attract attention due to the proximity of different ground states including antiferromagnetic spin density waves (SDW), unconventional superconducting (SC) and metallic states, and magnetic field-induced spin density wave (FISDW) states [1,2]. Recently, arguments have been made for the coexistence of the SDW, SC, and metallic states along phase boundaries [3–5], for the possibility that the metallic state is an unconventional SDW phase [6], and even for the survival of p-wave Cooper pairing in the metallic state [7].

Most studied are $(TMTSF)_2PF_6$ and $(TMTSF)_2ClO_4$. These materials are quasi-one-dimensional (Q1D) organic conductors with transfer integrals of order 250, 25, and 0.25 meV for the a, b, and c axis directions, respectively. In the SC state, for magnetic fields aligned in the ab conducting plane, the critical field H_{c2} exceeds the Pauli limit [8,9], and no change of the electron spin susceptibility in Knight shift is observed below T_c [10], suggesting p-wave pairing in these materials. Above H_{c2}, in the metallic state, ''Lebed magic angle'' effects [11] were first observed in $(TMTSF)_2ClO_4$ [12,13] [and later in $(TMTSF)_2PF_6$ [14]] as dips at magic angles in angular dependent magnetoresistance (ADMR) data for tilted magnetic field in the bc planes, perpendicular to the most conducting a axis. The magic angles occur when $\tan\theta \approx 1.1p/q$, where θ is the angle between the field and c axis, and p, q are integer values of the c and b unit cell parameters, respectively [12,13]. Above a threshold field H_{th}, the FISDW state (with a cascade of subphases) is stabilized due to the quantized nesting of the Q1D Fermi surface [1,15].

In this Letter, we examine the longitudinal [Seebeck or thermoelectric power (TEP)] and transverse (Nernst) thermoelectric effects in the metallic and FISDW phases in $(TMTSF)_2ClO_4$ (hereafter ClO_4). The Nernst effect, an analogue of the Hall effect, is the transverse voltage induced by a temperature gradient in a magnetic field. A large Nernst signal can be induced by a phase slip in the vortex state [16,17], while a very small Nernst effect is expected for quasiparticles in normal Fermi liquids with one charge carrier [18,19]. When more than one type of carrier is involved, the Nernst effect can be finite and of order $(k_B/e)(T/T_F)(\omega_c\tau)$, where k_BT_F is the Fermi energy, ω_c is the cyclotron frequency, and τ is the scattering time—estimated to be a few nV/K for the Bechgaard salts [20]. However, a giant ($\sim \mu$V/K) resonant Nernst effect in $(TMTSF)_2PF_6$ (hereafter PF_6) has been reported by Wu *et al.* [20]. Here large negative dips and positive peaks are observed as the field angle is swept through magic angles in a narrow range. The effect was originally attributed to an electrical current ''lock-in'' at the magic angle where metallic (''coherent'') behavior appears, and to nonmetallic (''non-Fermi liquid'') behavior away from the magic angle [20]. Currently, a model has been proposed by Ong *et al.* [7] involving finite Cooper pairing in the metallic phase. Here the symmetry of pairs of fluctuating pancake vortices in the crystallographic planes will be broken by induced vortex density for finite in-plane field away from the magic angle directions. This can account for the magnitude and resonant nature of the Nernst signals [7]. We find that ClO_4 exhibits a resonant Nernst effect not only in the metallic state, but also at higher fields in the FISDW state, with a greatly enhanced magnitude. These new findings place conditions on models proposed to explain the anomalous Nernst signal in these materials.

Superconductivity appears at ambient pressure in ClO_4 below $\sim$1 K when cooled slowly (10–15 mK/min in this work) through the anion ordering (AO) temperature $T_{AO} \sim$ 24 K. Here the tetrahedral ClO_4 anions order, doubling the unit cell along the b axis. Although no AO occurs in PF_6, pressures above 6 kbar are necessary in PF_6 to stabilize the metallic and superconducting ground states. Under these respective conditions, both materials exhibit a metal-to-FISDW transition above a threshold magnetic field ($H_{th} \sim$ 4 T for ClO_4 and $H_{th} \sim$ 7 T for PF_6 at 10 kbar) for $B \parallel c$. In the present work, the sample is placed in an evacuated

 © 2005 The American Physical Society

holder sealed at room temperature and the Nernst signal is measured along the b axis with $\Delta T \parallel a$ axis (Fig. 1). The sample is rotated around the a axis so that the magnetic field (either forward or reversed) is in the bc plane. The TEP (Nernst) signal is derived from $\Delta V_1/\Delta T$ ($\Delta V_2/\Delta T$), where ΔV_1 (ΔV_2) is the longitudinal (transverse) voltage drop and ΔT is the temperature gradient. The final results are obtained by averaging the signals from the positive and negative field runs assuming that the TEP (Nernst effect) is an even (odd) function of the magnetic field.

Figure 1 shows the angle dependence of the Nernst signal (N) at different fields at 0.4 K. The down arrows indicate the FISDW threshold angle ($\theta_{\rm th}$) determined by $H_\perp = H\cos\theta_{\rm th} = H_{\rm th}$, where $H_{\rm th}$ (about 3.9 T at 0.4 K) is the threshold field. Resonant Nernst signals are observed in both the metallic ($\theta > \theta_{\rm th}$) and FISDW ($\theta < \theta_{\rm th}$) states. The Nernst signal increases as the sample undergoes a phase transition between the metallic and FISDW states. In the FISDW state, additional structure related to the cascade of FISDW subphases appears as $H_\perp$ increases for $\theta \to 0$. For example, the positions of the dips above $H_\perp > H_{\rm th}$ (marked as short vertical lines) satisfies $H_\perp \sim$ 4.2 T. The anomalies due to the FISDW subphases will be discussed later. In contrast to the Nernst effect, the low temperature TEP signal does not show noticeable changes at magic angles in the metallic state as shown in the inset of Fig. 1.

In the metallic phase, the positions of dips at $-52°$ ($\theta_{m-}{}^{(1)}$), peaks at $-43°$ ($\theta_{m+}{}^{(1)}$) and zeros at $-48°$ ($\theta_m{}^{(1)}$) in Fig. 1 are field independent, and the midangle ($\theta_m{}^{(1)}$) is the magic angle for $p = q = 1$ where the field is along the $2b + c$ direction (consistent with anion ordering). Hence the resonantlike behavior with sign changes of the Nernst effect around the magic angle for ClO_4 is similar to that of PF_6 at 10 kbar [20]. For the magic angle $\theta_m{}^{(0)}$ for $B \parallel c^*$ the Nernst signal appears to be resonant (as it is in PF_6 where it is accessible below $H_{\rm th}$), but due to the lower $H_{\rm th}$ the additional complications of the FISDW subphases make systematic analysis difficult.

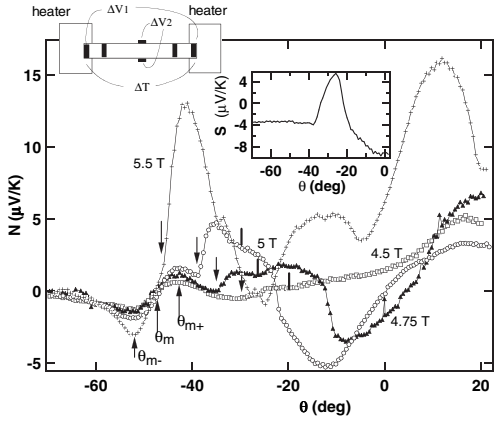

FIG. 1. Angle dependence of the Nernst signal at different fields at 0.4 K. See text for the meanings of arrows and vertical lines. Left inset: the contact configuration. Right inset: the angle-dependent TEP (S) at 0.4 K and 5 T.

The normalized peak-to-peak Nernst data ($N_{\rm pp}{}^N = N_{\rm pp}/H$) in the metallic state are shown in Fig. 2. For the values around $\theta_m{}^{(1)}$, $N_{pp}{}^N$ grows gradually, initially followed by an abrupt increase for fields higher than 4.5 T and temperatures lower than 0.8 K. This nonmonotonic behavior strongly suggests that normal Fermi liquid picture is not valid even in the metallic state. The maximum $N_{\rm pp}$ in ClO_4 is about 4 μV/K at 5.2 T and 0.4 K (for the first magic angle $\theta_m{}^{(1)}$), which is of same order of magnitude as PF_6 even though PF_6 was measured along the a axis with $\Delta T \parallel b$ axis [20].

The angular dependences of the Nernst effect at higher fields are presented in Fig. 3(a), where, in the inset, a summary of all data clearly shows the equivalence of the resonant Nernst periods for both metallic and FISDW phases. The resonant signal is evident for the second ($p/q = 2$) magic angle, and the positive peaks for the third ($p/q = 3$) magic angle is also observed. The up arrows indicate $\theta_{\rm th}$ and the down arrows show the angle below which the Nernst signal is angle independent. The down arrows follow $H_\perp = H\cos\theta$, where $H_\perp = 6.5$–6.9 T.

Additional structures due to the FISDW subphases also appear with the resonant behavior. In principle, the resonant Nernst signal can be differentiated from the FISDW subphases since the latter should occur at a certain $H_\perp$ while the former is depending only on angle. In Fig. 3(b), the angular dependence of the Nernst effect at selected fields from both Figs. 1 and 3(a) is plotted against $H_\perp$. There are two different features: (1) anomalies associated with the FISDW subphases whose positions do not change and (2) peaks and dips where the condition $H_\perp = H\cos\theta_{m+(-)}$ is satisfied. For some values of $H_\perp$ these features coincide, and this makes it difficult to isolate the resonant Nernst signal from the FISDW subphases. This also may influence the apparent width of the Nernst resonance, which may be smaller than it appears in the inset of

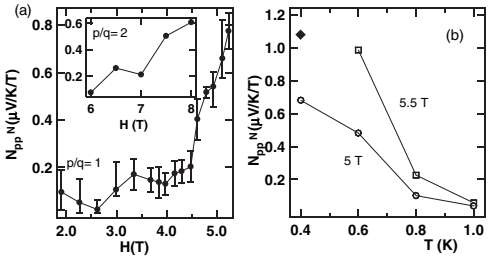

FIG. 2. The normalized peak-to-peak Nernst signal $[N(\theta_{m+}) - N(\theta_{m-})]/H$ in the metallic state. (a) Field dependence at 0.4 K for $p/q = 1$ and 2 (inset). (b) Temperature dependence at 5 K and 5.5 T. The data point at 0.4 K and 5.5 T (◆) is for the negative peak at $\theta = \theta_{m-}{}^{(1)}$ (since $\theta_{m+}{}^{(1)}$ was in the FISDW state).

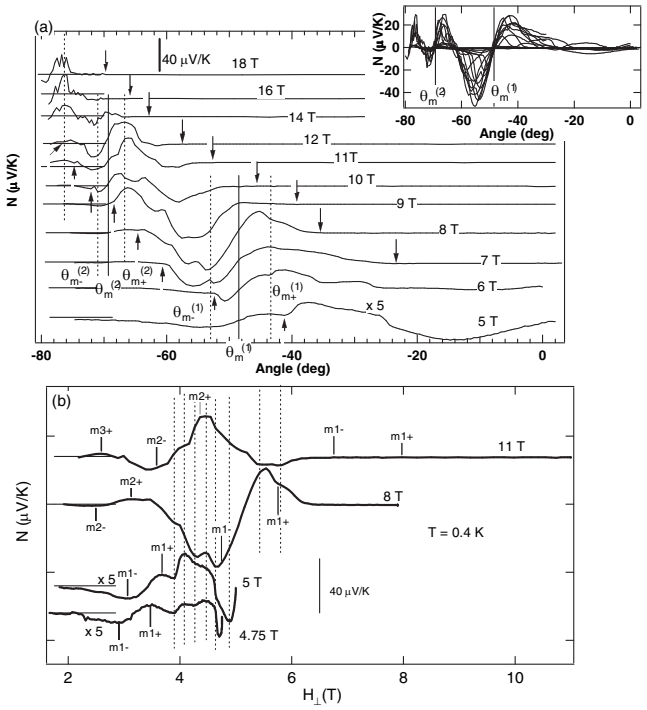

FIG. 3. (a) The angle dependence of the Nernst effect for representative fields, offset for clarity. The solid lines indicate the magic angles ($\theta_m{}^{(1)}$ for $p/q = 1$ and $\theta_m{}^{(2)}$ for $p/q = 2$) obtained from the ADMR measurements. The dotted lines indicate the angles where the Nernst signal shows a dip or peak in the metallic state. Inset: Nernst data for all fields between 5 and 18 T without offset. (b) The Nernst signal as a function of $H_\perp$, offset for clarity. The dotted vertical lines indicate anomalies associated the FISDW transitions. The resonant Nernst signals are labeled as $mn + (-)$ indicating peaks (dips) at $p/q = n$ magic angles.

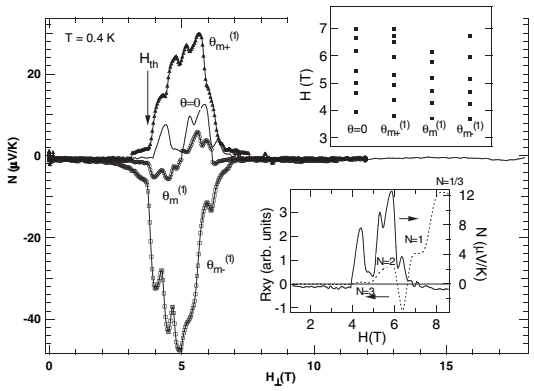

FIG. 4. The Nernst signal as a function of $H_\perp (= H\cos\theta)$. Upper inset: positions of dips at different angles. Lower inset: Hall resistance and Nernst effect on the same sample for $\theta = 0$.

Fig. 3(a). If we compare the width of the resonance in the metallic state where the subphase effect is absent, the peak-to-peak angle ($\theta_{m+} - \theta_{m-}$) is $\sim 9°$ in ClO_4 and $\sim 5°$ in PF_6.

In Fig. 4, the field dependence of the Nernst effect is shown for fixed angles $\theta = 0$, $\theta_{m+}{}^{(1)}$, $\theta_m{}^{(1)}$, and $\theta_{m-}{}^{(1)}$ vs $H_\perp = H\cos\theta$. For $\theta = \theta_{m+}$ and θ_{m-}, the resonant Nernst signal becomes apparent above $H_\perp = 2.3$ T for $\theta = \theta_{m-}$ and 3.1 T for $\theta = \theta_{m+}$ in the metallic state. In the FISDW state above H_{th}, the Nernst signal changes sign for small variations around the magic angle, and its magnitude at $\theta = \theta_{m-}$ and θ_{m+} is even larger than at $\theta = 0°$. Even when the Nernst signal changes sign, the FISDW subphase transitions are clear at all angles, as shown in the upper inset of Fig. 4. At higher fields above $H_\perp = 6.5$–6.9 T, the Nernst effect is small for any field direction. Although perhaps coincidental, this field is in the range where the Hall resistance makes its last sign reversal above the Ribault anomaly [21] and enters the positive Hall ($N = 1$) state as shown in the lower inset of Fig. 4. The high field resonant Nernst signal for $H \parallel c^*$ is also suppressed in PF_6, when the sample is in the FISDW state (0.2 K, $H_\perp = 7.5$ T) [20].

In the metallic phase, ClO_4 and PF_6 show a similar resonant Nernst behavior around magic angles, even with anion ordering in the case of ClO_4, and even though the present and previous studies were for the off-diagonal and diagonal configurations, respectively [22]. This includes similarities in the amplitude and the field and temperature dependence of N_{pp}. We have further shown that the resonant Nernst effect persists in the FISDW phase of ClO_4 in fields up to $H_\perp \sim 6.9$ T.

There are several puzzles: the large value of the Nernst effect in the ''metallic state'' in magnetic fields and what type of excitation, superconducting vortex, or otherwise, is acting, its enhancement in the FISDW state, the resonant nature of the Nernst signal, and its ultimate attenuation in higher magnetic fields. Based on previous transport studies, several key factors of the problem appear to be well established, namely, that for fields along magic angles there is coherent, metallic transport, and away from the magic angles the transport shows non-Fermi liquid behavior [23]. Combined with independent spectroscopic investigations [24], which show that both PF_6 and ClO_4 lie in a regime close to dimensionality crossover between 1D non-Fermi liquid and 2D Fermi liquid behavior, the possibility that the magnetic field stabilizes the 2D Fermi liquid at the magic angles, but drives the system into an incoherent state away from magic angles, is not unreasonable [25]. Moreover, recent theoretical work has shown that dimensional crossover predicts the dips in the ADMR at the magic angles without invoking superconductivity [26]. In addition, for fields aligned near magic angles, coherent currents between chains of some form can in principle lead to Lorentz-type forces that would produce resonant transverse (Nernst or Hall) signals.

In addition to the high T_c cuprates [17], there are reports of large (although nonresonant) Nernst effects in organic [27,28] and inorganic [29,30] materials. In these materials

the large Nernst effects were attributed to the quasiparticles, rather than vortices, in the density wave states [28,29] or near the quantum critical point [30]. Hence in the case of the Bechgaard salts, it is possible that a nonsuperconducting mechanism leads to the large value of the Nernst signal. An unconventional spin density wave (USDW) theory [6] has been proposed to describe the metallic state in PF_6. Although the USDW theory yields the Nernst effect, peaks, and not resonant structures, are predicted at the magic angles in this model.

In light of the above discussion, the superconducting vortex model is attractive since it provides excitations that not only yield a resonant Nernst signal and smaller nonresonant Seebeck amplitude, but also carry high entropy that produces large Nernst amplitude. However, there are several aspects of the vortex model that need to be addressed. The condition $N \gg S_{xx}$ discussed by Ong *et al.* [7] for PF_6 under pressure suggests that vortex flow causes the Nernst signal. However, in all studies of the S_{xx} on ClO_4 in the standard longitudinal configuration in vacuum of which we are aware [31] including our own, S_{xx} is of the order 2 to 4 μV, so the condition $N \gg S_{xx}$ is not strictly satisfied. Furthermore, the angular dependence of S_{xx} does not show any noticeable changes at the magic angles, and, recent ^{77}Se NMR investigations [32] show no systematic change in the spin-relaxation rate for rotations through the magic angles.

The Nernst effect signal in the FISDW state can be modeled by considering two parallel conduction channels, one from the nested gapped Fermi surface and the other from electron or hole carriers responsible for the Landau quantization [33]. The former carriers should be activated across the gap, so the resistance and thermoelectric tensor will be divergent with decreasing temperature, while the latter carriers may retain the character of the metallic state. The total Nernst effect will be $N_{\text{total}} = (\sigma_{\text{FISDW}} N_{\text{FISDW}} + \sigma_{\text{Metal}} N_{\text{Metal}})/(\sigma_{\text{FISDW}} + s_{\text{Metal}})$, where σ_{FISDW} (σ_{Metal}) and N_{FISDW} (N_{Metal}) represent conductivity and Nernst signal in the FISDW (metallic) state, respectively. Since the contribution to the total Nernst effect of the FISDW carriers is the weighted by their conductivity, the behavior of the metallic carriers may survive in the FISDW state. The suppression of the Nernst signal at higher fields may be explained if one assumes σ_{FISDW} becomes very small at that field region. Another model to explain the suppression involves collective transport (no heat current accompanying the electrical current) when the FISDW state is stabilized at higher fields [33].

In summary, we find the resonant Nernst effect is a general feature of several members of the Bechgaard salts in both their metallic and FISDW phases, where comparisons can be made. The coherent-incoherent picture at or near magic angle planes seems to be a robust description, based on both experimental and theoretical treatments. What remains to be settled is the nature of the excitations that are present in the 2D planes which cause the large Nernst signal. Our finding that when the FISDW gap opens the Nernst signal is enhanced suggests that electron and hole excitations in the presence of an energy gap may provide the mechanism for a large Nernst signal, without the need to invoke superconductivity. Even in the metallic state, a ''correlation gap'' [24] should appear away from the magic angles that could enhance the Nernst signal. We note that high sensitivity torque magnetization and Hall effect measurements at the magic angles would be useful to advance our understanding of this phenomena, since in the case of a vortexlike excitation, both should show resonant behavior. At present torque [12] and Hall [14] measurements are still inconclusive in this respect.

We wish to thank M. Naughton, P. Chaikin, and W. Wu for helpful comments concerning this work. This work is supported by NSF 02-03532 and the NHMFL is supported by the National Science Foundation and the State of Florida. The work at Ewha University is supported by KOSEF R01-2003-000-10470-0(2004).

[1] P. M. Chaikin, J. Phys. I (France) **6**, 1875 (1996).
[2] T. Ishiguro, K. Yamaji, and G. Saito, *Organic Superconductors II* (Springer-Verlag, Berlin, 1998).
[3] T. Vuletic *et al.*, Eur. Phys. J. B **25**, 319 (2002).
[4] A. V. Kornilov *et al.*, Phys. Rev. B **69**, 224404 (2004).
[5] D. Podolsky *et al.*, Phys. Rev. Lett. **93**, 246402 (2004).
[6] B. Dóra *et al.*, Europhys. Lett. **67**, 1024 (2004).
[7] N. P. Ong *et al.*, Europhys. Lett. **66**, 579 (2004).
[8] I. J. Lee *et al.*, Phys. Rev. Lett. **78**, 3555 (1997).
[9] J. I. Oh *et al.*, Phys. Rev. Lett. **92**, 067001 (2004).
[10] I. J. Lee *et al.*, Phys. Rev. Lett. **88**, 017004 (2002).
[11] A. G. Lebed, JETP Lett. **43**, 174 (1986).
[12] M. J. Naughton *et al.*, Phys. Rev. Lett. **67**, 3712 (1991).
[13] T. Osada *et al.*, Phys. Rev. Lett. **66**, 1525 (1991).
[14] W. Kang *et al.*, Phys. Rev. Lett. **69**, 2827 (1992).
[15] L. P. Gor'kov *et al.*, J. Phys. (France) **45**, L433 (1984).
[16] Y. Wang *et al.*, Science **299**, 86 (2003).
[17] Z. A. Xu *et al.*, Nature (London) **406**, 486 (2000).
[18] E. H. Sondheimer, Proc. R. Soc. London **193**, 484 (1948).
[19] Y. Wang *et al.*, Phys. Rev. B **64**, 224519 (2001).
[20] W. Wu *et al.*, Phys. Rev. Lett. **91**, 056601 (2003).
[21] M. Ribault, Mol. Cryst. Liq. Cryst. **119**, 91 (1985).
[22] A similar behavior, with another off-diagonal configuration ($\Delta T \parallel a$ axis, $\Delta V_2 \parallel c$ axis), is also found in PF_6 (W. Wu, Ph.D. thesis, Princeton University, 2004).
[23] E. I. Chashechkina *et al.*, Phys. Rev. Lett. **80**, 2181 (1998).
[24] V. Vescoli *et al.*, Science **281**, 1181 (1998).
[25] S. P. Strong *et al.*, Phys. Rev. Lett. **73**, 1007 (1994).
[26] A. G. Lebed *et al.*, Phys. Rev. Lett. **93**, 157006 (2004).
[27] E. S. Choi *et al.*, Phys. Rev. B **65**, 205119 (2002).
[28] B. Dóra *et al.*, Phys. Rev. B **68**, 241102(R) (2003).
[29] R. Bel *et al.*, Phys. Rev. Lett. **91**, 066602 (2003).
[30] R. Bel *et al.*, Phys. Rev. Lett. **92**, 217002 (2004).
[31] R. C. Yu *et al.*, Phys. Rev. Lett. **65**, 2458 (1990).
[32] W. Wu *et al.*, Phys. Rev. Lett. **94**, 097004 (2005).
[33] W. Kang *et al.*, Phys. Rev. B **45**, 13 566 (1992).